J. Biochem. **134**, 403–413 (2003)
DOI: 10.1093/jb/mvg158

High-Level Expression of Porcine Liver Cytochrome P-450 Reductase Catalytic Domain in *Escherichia coli* by Modulating the Predicted Local Secondary Structure of mRNA

Shigenobu Kimura* **and Takashi Iyanagi**

Department of Life Science, Graduate School of Science, Himeji Institute of Technology, Kouto 3-2-1, Kamigori, Hyogo 678-1297

Received May 22, 2003; accepted June 24, 2003

A direct expression system for the solubilized catalytic domains of NADPH-cytochrome P-450 reductase (sCPR) from rat (RsCPR) and porcine (PsCPR) in *Escherichia coli* cells was constructed using the expression plasmid pCWori+. PsCPR was minimally expressed, whereas RsCPR was highly expressed. Replacement of the nucleotides encoding $Thr^{60}Ser^{61}Ser^{62}$ in PsCPR with those for $Ala^{60}Pro^{61}Pro^{62}$ in RsCPR markedly increased the expression level of the protein. The local secondary structures of the mRNAs, which were predicted with the prediction program GeneBee (http://www.genebee.msu.su), suggested that the intramolecular double strand between the ribosome binding site (RBS) and the $Thr^{60}Ser^{61}Ser^{62}$ codons in PsCPR, and/or the base-pairing at the initiation codon of the mRNAs significantly affected protein expression. Silent mutations were systematically introduced into the codons for Thr^{58} and $Thr^{60}Ser^{61}$ in PsCPR to modulate the local secondary structure of the mRNA. The expression level of the silently mutated PsCPR suggests that the expression level of PsCPR depends on the stability of the local structure at the RBS in the mRNA. A high-level expression system for wild-type PsCPR was constructed by introducing silent mutations at the codons for $Thr^{60}Ser^{61}$ in PsCPR. The purified PsCPR showed the characteristic absorption spectral changes of sCPR after reduction with NADPH. The yield of purified PsCPR from 1 liter of culture fluid was 45.8 mg. These results substantiate that the introduction of silent mutations in the section of the gene encoding the N-terminal region of the protein based on the predicted local secondary structure of the mRNA at the RBS is a useful approach to control and increase the expression level of heterologous proteins in *E. coli* cells.

Key words: mRNA, NADPH-cytochrome P-450 reductase, ribosome binding site, secondary structure prediction, Shine-Dalgarno sequence.

Abbreviations: RBS, ribosome binding site; CPR, NADPH-cytochrome P-450 reductase; sCPR, solubilized catalytic domain of CPR; PsCPR, porcine liver sCPR; RsCPR, rat liver sCPR; Psb5R, solubilized catalytic domain of porcine liver NADH-cytochrome b_5 reductase; Psb5, solubilized domain of porcine liver cytochrome b_5; IPTG, isopropyl-β-D-thiogalactopyranoside; CBB, Coomassie Brilliant Blue R-250; bp, base pairs.

Heterologous gene expression using recombinant DNA techniques is necessary for the identification, characterization, and *in vitro* studies of the biologically active forms of proteins that are seldom prepared from natural sources. In addition, high expression systems for heterologous genes in *Escherichia coli* have become increasingly important with recent progress in comprehensive studies of so-called "proteomes." Although *E. coli* cells do not have the same posttranscriptional modification systems as those of eukaryotic cells, heterologous gene expression in *E. coli* cells has the following advantages: (i) gene manipulation techniques are well established in *E. coli*, (ii) a large amount of protein can be synthesized in a short time, and (iii) fermentation scale up of *E. coli* cells is much easier than with eukaryotic cells.

It is well known that the amount of heterogeneous proteins produced by *E. coli* cells depends on various factors, such as the copy number and stability of the expression plasmid in the cells, the synthetic level and stability of mRNA, the efficiency of polypeptide synthesis, and the stability of the synthesized proteins in *E. coli* cells (*1*). Various plasmid vectors have been designed and widely used for the high-level expression of heterologous genes in *E. coli* cells**.** Most of these expression plasmids contain a high-copy number origin of replication (such as ColEI), strong promoters (such as *trp, lac, tac*, λP_L, and *T7*) and the appropriate regulatory elements to synthesize large amounts of mRNA (*2*, *3*), and a ribosome binding site (RBS; also known as the Shine-Dalgarno sequence) (*4*). However, the levels of recombinant proteins produced in *E. coli* cells depend on the individual proteins. Therefore, various problems typically have to be overcome on a case by case basis in order to realize high-level expression (*5*–*9*).

The specific electron transfer system on the endoplasmic reticulum in hepatocytes, which consists of NADH-cytochrome b_5 reductase, cytochrome b_5, and NADPH-cytochrome P-450 reductase (CPR), participates in physiological fatty acid synthesis, cholesterol synthesis, and

*To whom correspondence should be addressed. Tel: +81-791-58-0207, Fax: +81-791-58-0132, E-mail: s-kimura@sci.himeji-tech.ac.jp

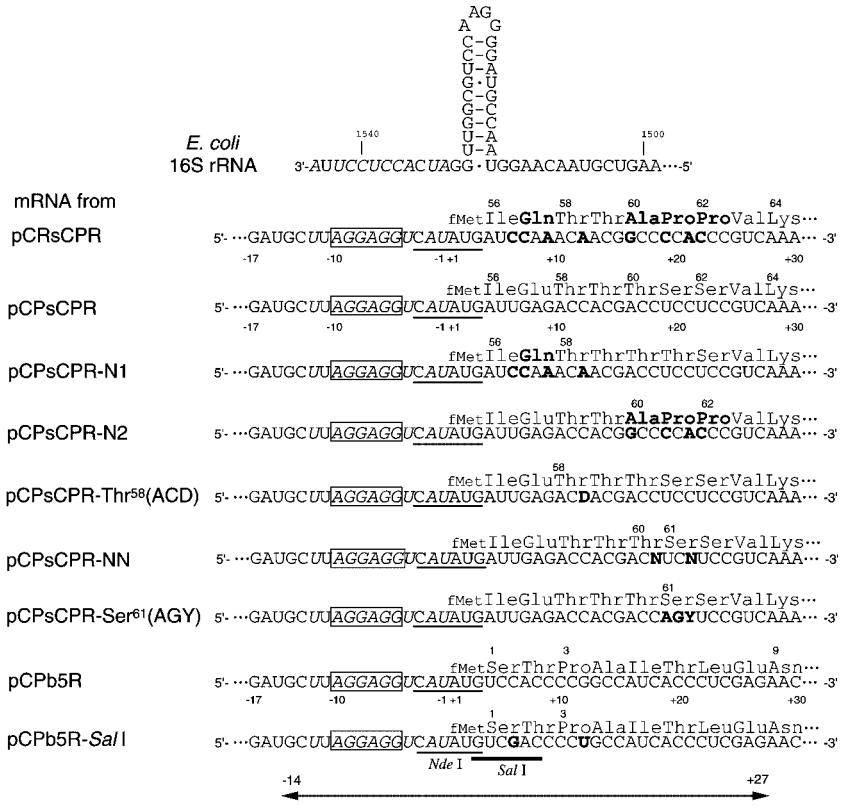

Fig. 1. **Partial nucleotide sequences of the mRNAs from the expression plasmids for sCPRs and the nucleotide sequence at the 3′-terminal region of *E. coli* 16S rRNA.** Secondary structure of *E. coli* 16S RNA in the region 1499–1544 and partial nucleotide sequences of mRNAs are shown with the deduced amino acid residues. The plasmid that produces the mRNA is shown at the left of the partial nucleotide sequence. The amino acid numbers are located above the amino acid sequences, and the nucleotide numbers are below the nucleotide sequences. The nucleotides that are complementary between the upstream of the initiation codon (AUG) encoding formylmethionine (fMet) in the mRNAs and the 3′-terminal region of *E. coli* 16S rRNA are shown in italics. The hypothetical RBS (AGGAGG) is boxed. The amino acid residues and nucleotides in the mRNA from pCRsCPR that are not conserved with those from pCPsCPR, those from pCRsCPR-N1 and -N2 that are identical to those in the mRNA from pCRsCPR, and the nucleotides in mRNA from pCPsCPR-Thr^{58}(ACD), -NN, -C(AGY), and pCPb5R-*Sal*I that were silently mutated are shown in bold letters. In the nucleotide sequence, D represents either A, U, or G, N represents A, U, G, or C, and Y represents U or C. The nucleotide sequences with thin and thick underlining correspond to the *Nde*I and *Sal*I sites in the expression plasmids, respectively. The arrow at the bottom of the figure indicates the region of the nucleotide sequence between –14 to +27 that was used for secondary structure prediction.

oxidation of xenobiotic compounds. In this system, CPR [EC 1.6.2.4] mediates the specific electron transfer from NADPH to cytochrome P-450, cytochrome b_5, microsomal heme oxygenase, and fatty acid elongase (*10*). CPR is a membrane-bound protein that contains both an FAD and an FMN in each molecule, and shows characteristic spectral changes after successive reductions with NADPH (*11*). The tertiary structures of the solubilized catalytic domains of NADH-cytochrome b_5 reductase, cytochrome b_5, and CPR derived from various mammalian species have been determined by X-ray analysis (*12–16*). Based on the tertiary structures, various mutagenesis studies addressing the specific recognition and regulation mechanisms of electron transfer among these proteins have been carried out (*15*, *17–25*). However, specific details of the electron transfer among these proteins have not yet been clearly elucidated. The study of physiologically relevant combinations of recombinant proteins derived from the same source is a good approach to elucidate the precise mechanism of specific intermolecular recognition and electron transfer. Therefore, we have planned to reconstruct an *in vitro* electron transfer system using recombinant solubilized catalytic domains of these proteins from a single source, porcine liver. We previously cloned the cDNAs encoding the solubilized catalytic domains of porcine liver NADH-cytochrome b_5 reductase (Psb5R) and the solubilized domain of cytochrome b_5 (Psb5). Both genes were highly expressed in *E. coli* cells using the expression vector pCW$_{ori}^+$ (*18*, *20*). Plasmid pCW$_{ori}^+$ contains two tandem *tac* promoters and a RBS, which is highly complementary to the 3′-end region of the 16S rRNA in the 30S subunit of *E. coli* (Fig. 1). Expression is under the control of the *cI* repressor (*26*, *27*). This plasmid has been widely used for the high-level expression of various electron transfer proteins such as cytochrome P-450 17α-hydroxylase, nitric oxide synthase, and its flavin domain (*28–30*).

In this study, we cloned a cDNA encoding porcine sCPR (PsCPR) and constructed an expression plasmid for PsCPR using pCW$_{ori}^+$. Interestingly, we found that the level of PsCPR produced in *E. coli* cells is very low, although that of the corresponding domain of rat CPR (RsCPR) is very high. We demonstrate here that differences in the amino acid and/or nucleotide sequences of the N-terminal/5′ regions between PsCPR and RsCPR are critical for determining the accumulation levels of the proteins. In addition, modulation of the predicted local secondary structure at the RBS in the mRNA markedly increased the accumulation level of the recombinant PsCPR in *E. coli* cells. Finally, we discuss the usefulness of introducing silent mutations into the part of the gene encoding the N-terminal region of the protein based on the local secondary structure prediction of mRNA at the RBS for controlling the expression level of heterologous proteins in *E. coli* cells.

MATERIALS AND METHODS

Materials—Enzymes for recombinant DNA technology were from Takara and Toyobo. *E. coli* strain BL21 [F$^-$ *ompT hsdS*$_B$ ($r_B^-m_B^-$) *gal dcm*] was from Novagen. Plasmid pCW$_{ori}^+$ was kindly provided by Dr. F. W. Dahlquist at the University of Oregon. Plasmid pTRF2, which contains cDNA encoding rat CPR, was from Sumitomo.

Construction of pCPsCPR—The cDNA encoding PsCPR was amplified from the first strand cDNA, previously prepared from porcine liver (*18*), by PCR using the forward primer 5′-AGGAGGTCATATGATTGAGACCAC-GACC-3′ (primer-1), which has an *Nde*I site (underlined) containing an additional initiation codon (italics), followed by the nucleotide sequence encoding from Ile^{56} to Thr^{60} of the porcine CPR gene (EMBL Data Bank accession no. L33893), and the reverse primer 5′-CCGCCAAG-CTT*CTACTA*GCTCCAGACGTC-3′ (primer-2), which corresponds to the C-terminal tetrapeptide of the porcine CPR, two stop codons (italics), and a *Hin*dIII site (underlined). Amino acid numbering starts from the acetylated N-terminal glycine residue (*31*). The resultant fragment was inserted into pCW_{ori}^+ using *Nde*I and *Hin*dIII sites to construct the expression plasmid pCPsCPR. The plasmid pCPsCPR contains the nucleotide sequence encoding 622 amino acid residues from Ile^{56} to Ser^{677} of porcine CPR. The deduced amino acid sequence is identical to that previously determined by amino acid sequence analysis of natural PsCPR (*32*).

Construction of pCRsCPR—The DNA fragment encoding RsCPR was amplified from the gene encoding rat CPR in the plasmid pTRF2 using the forward primer 5′-AGGAGGTCATA*TG*ATCCAAACAACGGCC-3′, which has an *Nde*I site (underlined) containing an additional initiation codon (italics), followed by the nucleotide sequence encoding from Ile^{56} to Ala^{60} of rat CPR (*33*), and the reverse primer 5′-CCGCCAAGCTTCTAGCTCCACAC-ATC-3′, which corresponds to the C-terminal tetrapeptide of rat CPR, a stop codon (italics), and a *Hin*dIII site (underlined). The resultant fragment was inserted into pCW_{ori}^+ using *Nde*I and *Hin*dIII sites to construct pCRsCPR.

Construction of pCPsCPR-N1 and -N2—The DNA encoding PsCPR-N1, in which the nucleotide sequence encoding $Ile^{56}Glu^{57}Thr^{58}$ in PsCPR was replaced with that encoding $Ile^{56}Gln^{57}Thr^{58}$ in RsCPR, was prepared from the DNA template pCPsCPR by PCR using a mutagenic forward primer 5′-AGGAGGTCATATG**ATC-CAAACA**ACGACCTCCTCCGTC-3′, which has an *Nde*I site (underlined) and the nucleotide sequence encoding $Ile^{56}Gln^{57}Thr^{58}$ in RsCPR (bold), and primer-2. The resultant fragment was inserted into pCW_{ori}^+ using *Nde*I and *Hin*dIII sites to construct pCPsCPR-N1. The DNA encoding PsCPR-N2, in which the nucleotide sequence encoding $Thr^{60}Ser^{61}Ser^{62}$ in PsCPR was replaced with that encoding $Ala^{60}Pro^{61}Pro^{62}$ in RsCPR, was prepared by two rounds of PCR. First, a mutated DNA fragment was prepared from pCPsCPR using the mutagenic forward primer 5′-CG**GCCCCACCC**GTCAAAGACAGCAG-CTTC-3′, which has the nucleotide sequence encoding $Ala^{60}Pro^{61}Pro^{62}$ in RsCPR (bold), and primer-2. The resultant fragment was purified and reamplified with the approximately 330 base pairs (bp) *Bam*HI–*Nde*I–*Pst*I fragment of pCPsCPR, the forward primer 5′-CCGGATC-CATCGATGCTTAGG-3′, which has the nucleotide sequence of pCW_{ori}^+ containing a *Bam*HI site (underlined) at upstream of the *Nde*I site, and primer-2. The amplified fragment was inserted into pCW_{ori}^+ using *Bam*HI and *Hin*dIII sites to construct pCPsCPR-N2. The entire nucleotide sequences of the mutated genes were confirmed by nucleotide sequencing using an ABI PRISM 310 Genetic Analyzer.

Silent Mutations in the PsCPR Gene—The expression plasmids pCPsCPR-Thr^{58}(ACA), -Thr^{58}(ACT), and -Thr^{58}(ACG), in which the nucleotides ACC encoding Thr^{58} in pCPsCPR were silently mutated to ACA, ACT, and ACG, respectively (Fig. 1), were constructed by PCR from pCPsCPR using the mixed mutagenic forward primer 5′-AGGAGGTCATATGATTGAG**ACD**ACGACCTC-3′, which has an *Nde*I site (underlined) and the nucleotides encoding Thr^{58} in PsCPR (bold), and primer-2. In this case, base D is a mixture of A, G, and T. The resultant mixture of PCR products was inserted into pCW_{ori}^+ using *Nde*I and *Hin*dIII sites. *E. coli* BL21 cells were transformed with the resultant mixture of plasmids. Transformants containing pCPsCPR-Thr^{58}(ACC), -Thr^{58}(ACT), and Thr^{58}(ACG) were identified by nucleotide sequence analysis of the plasmids.

The plasmids pCPsCPR-NN and -Ser^{61}(AGY) were constructed as follows. The former plasmid had silent mutations encoding $Thr^{60}Ser^{61}$ (ACCTCC to ACNTCN), and the latter plasmid had silent mutations encoding Ser^{61} (TCC to AGY). In these nucleotide sequences, N is either A, G, C, or T, and Y is C or T. Therefore, the plasmid pCPsCPR can be designated as pCPsCPR-CC (Fig. 1). At first, random silent mutations were introduced into pCPsCPR by PCR using the random mutagenic primer 5′-**GATTGAGACCACG**ACNTCNTCCGTCAAAGACAGC-3′ (primer-3), which has an identical nucleotide sequence to the 3′-terminal region of primer-1 (bold), and primer-2. The base N indicates a mixture of A, G, C, and T. The resultant PCR product was extended to the 5′-end by reamplification with primer-1 and primer-2, and inserted into pCW_{ori}^+ using *Nde*I and *Hin*dIII sites. *E. coli* BL21 cells were transformed with the mixture of the resultant plasmids. Ten different clones were selected from 28 single colonies of transformants by nucleotide sequence analysis of the plasmids. The plasmids pCPsCPR-AA and -AT, -TG and -CG, -CA, -GC, -Ser^{61}(AGC), and -Ser^{61}(AGT), were prepared by the same method except for the use of mutagenic primers, in which ACNTCN in primer-3 encoding $Thr^{60}Ser^{61}$ was replaced with ACATCW, ACYTCG, ACCTCA, ACGTCC, ACCAGC, and ACCAGT, respectively. The nucleotide W represents a mixture of A and T, and the nucleotide Y is a mixture of T and C.

Expression and Analysis of Protein Accumulation—The sCPR genes were expressed in *E. coli* BL21 cells. The cells containing the expression plasmids were cultivated in 2× YT medium containing 50 μM ampicillin with shaking at 37°C overnight, and inoculated into Luria-Bertani (LB) medium containing 50 μM ampicillin at a ratio of 1/200 (v/v). After cultivation with shaking for 1.5 h at 37°C, isopropyl-β-D-thiogalactopyranoside (IPTG) was added to a final concentration of 0.2 mM, and cultivation was continued for 8 h.

Protein accumulation in the cells was analyzed by SDS-PAGE. Cells were harvested, dissolved in sample buffer (50 mM Tris-HCl (pH 6.8), 2% (w/v) SDS, 10% (w/v) glycerol, 5% (w/v) 2-mercaptoethanol, 0.05% (w/v) bromophenol blue, and 25 mM EDTA), and boiled for 3 min at 100°C. The whole cell extract of *E. coli* cells corresponding to 25 μl of *E. coli* cell culture was electro-

phoresed. After electrophoresis, proteins were stained with Coomassie Brilliant Blue (CBB) R-250 (Fulka). The accumulation level of the expressed protein was analyzed by densitometry. The CBB-stained gel was scanned with an EPSON scanner GT8700F. The intensity of the expressed PsCPR band was analyzed using NIH Image (ver. 1.6.2) by subtracting the intensity of the same position and area of bands from *E. coli* BL21/pCWori$^+$ on the same gel as a background. The whole cell extract of BL21/pCPsCPR-TT was used as a standard, and the relative intensity of the band of expressed PsCPR was calculated as a ratio to the band of the standard. Western blots were performed on nitrocellulose membranes, and translated proteins were detected with rabbit antibodies against natural RsCPR, which also recognize PsCPR, alkaline phosphate-linked goat-anti rabbit antibodies (Sigma), and the alkaline phosphatase color reaction using 5-bromo-4-chloro-3-indolyl phosphate.

mRNA Secondary Structure Prediction—The local secondary structure of mRNA was predicted with GeneBee (*34*, *35*), which is a program package for biopolymer structure analysis available on the Web (http://www.genebee.msu.su). The values of the cluster factor, conserved factor, compensated factor, conservativity, greedy parameter, and energy threshold were 2, 2, 4, 0.8, 2, and –4.0 kcal/mol, respectively.

Purification of sCPR—Wild-type RsCPR and PsCPR were purified from *E. coli* BL21 cells containing pCRsCPR (BL21/pCPsCPR) and pCPsCPR-TT (BL21/pCPsCPR-TT), respectively. The cells, which were cultivated in LB medium containing 50 μM ampicillin and 0.2 mM IPTG for 16 h at 30°C, were lysed by sonication in 10 mM Tris-HCl (pH 7.4) containing 1 mM EDTA, 5% (w/v) glycerol, and 2 mM phenylmethylsulfonyl fluoride. The lysate was subjected to centrifugation at 18,000 ×*g* for 20 min, and the supernatant was applied to an anion exchange resin (DE52) column equilibrated with 10 mM potassium phosphate (pH 7.0) containing 1 mM EDTA (buffer A). Proteins were eluted with a linear gradient of sodium chloride from 0 to 0.5 M in buffer A. The fractions containing sCPR were applied to a 2′,5′-ADP Sepharose (Pharmacia) column equilibrated with buffer A containing 0.2 M sodium chloride (buffer B). The column was washed with buffer B, and sCPR was eluted with buffer B containing 10 mM 2′- and 3′-AMP mixture (Sigma). Fractions containing sCPR were diluted 3-fold with buffer A, and applied to a DE52 column equilibrated with buffer A. The column was washed with buffer A, and the absorbed sCPR was oxidized on the column by buffer A containing 25 mM potassium ferricyanide. The oxidized sCPR was eluted with buffer A containing 0.3 M sodium chloride, and desalted on a Sephadex G-25 (fine) (Pharmacia) column equilibrated with 100 mM potassium phosphate (pH 7.0) containing 1 mM EDTA.

Silent Mutation in the Pb5R Gene—The gene encoding Pb5R in pCPb5R (*18*) was mutated by PCR using the mutagenic forward primer 5′-GGAGGTCCATA*TGTCG*A-CCCC**T**GCCATCACC-3′, which has an *Nde*I site (underlined), a newly introduced *Sal*I site (italics), and nucleotides for the Ser^1 and Pro^3 silent mutations (bold), and the reverse primer 5′-CCGGATCC*TCTAGA*AGGCGAAGCAGC-3′, which corresponds to the C-terminal peptide of Pb5R followed by a stop codon (italics) and a *Xba*I site (underlined). The resultant fragment was inserted into pCW$_{ori}^+$ using *Nde*I and *Xba*I sites to construct pCPb5R-*Sal*I. The entire nucleotide sequence of the mutant gene was confirmed by nucleotide sequencing.

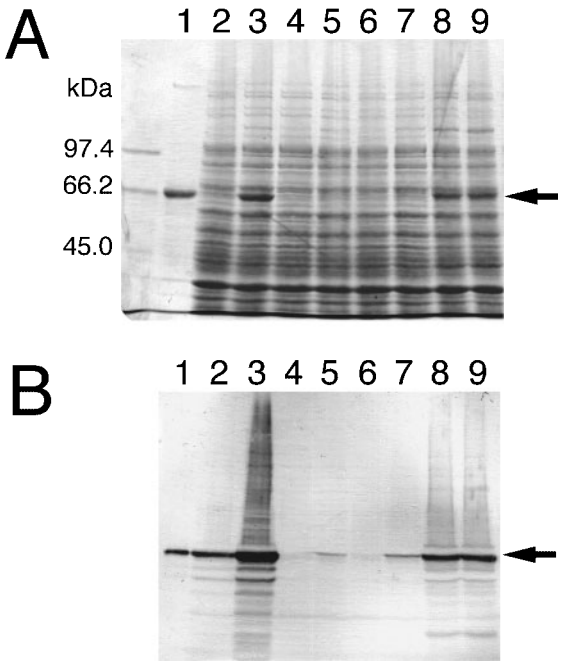

Fig. 2. **SDS-PAGE and Western blot analysis of *E. coli* whole cell extracts.** A: 7.5% polyacrylamide gel stained with CBB after SDS-PAGE. Purified RsCPR (1 μg), and the whole cell extract of 50 μl of *E. coli* culture fluid were analyzed. Markers are SDS-PAGE Molecular Weight Standards (Bio-Rad) including rabbit muscle phosphorylase *b* (97.4 kDa), bovine serum albumin (66.2 kDa), hen egg ovalbumin (45.0 kDa), bovine carbonic anhydrase (31.0 kDa), bovine pancreatic trypsin inhibitor (21.5 kDa), and hen egg lysozyme (14.4 kDa). B: Nitrocellulose membrane immuno-stained with rabbit antibodies against natural RsCPR and the alkaline phosphatase color reaction using 5-bromo-4-chloro-3-indolyl phosphate. The purified RsCPR (0.1 μg) and whole cell extracts from 5 μl of *E. coli* culture fluid were analyzed. In both A and B, purified RsCPR (*lane 1*), whole cell extracts of *E. coli* BL21/pCRsCPR (lanes 2 and 3), pCPsCPR (lanes 4 and 5), pCPsCPR-N1 (lanes 6 and 7), and pCPsCPR-N2 (lanes 8 and 9) cultivated for 8 h in the absence (lanes 2, 4, 6, and 8) or presence of 0.2 mM IPTG (lanes 3, 5, 7, and 9) were subject to electrophoresis. The position of the expressed sCPRs are shown with an arrow.

RESULTS

Expression of the Wild-type RsCPR and PsCPR Genes—The expression plasmids containing the wild-type RsCPR gene (pCRsCPR) and the PsCPR gene (pCPsCPR) were constructed using pCW$_{ori}^+$ (Fig. 1). The accumulation of RsCPR and PsCPR in *E. coli* BL21 cells containing pCRsCPR (BL21/pCRsCPR) and pCPsCPR (BL21/pCPsCPR) were analyzed (Fig. 2). Whole cell extracts of *E. coli* BL21/pCRsCPR produced after cultivation for 8 h in the presence of IPTG showed an obvious band at the same position as the purified RsCPR on a SDS-PAGE gel (Fig. 2A, lanes 1 and 3). In the presence of anti-RsCPR antibodies, this band was markedly and specifically immuno-stained (Fig. 2B, lane 3). These results indicate that RsCPR is highly expressed in *E. coli* BL21/pCRsCPR

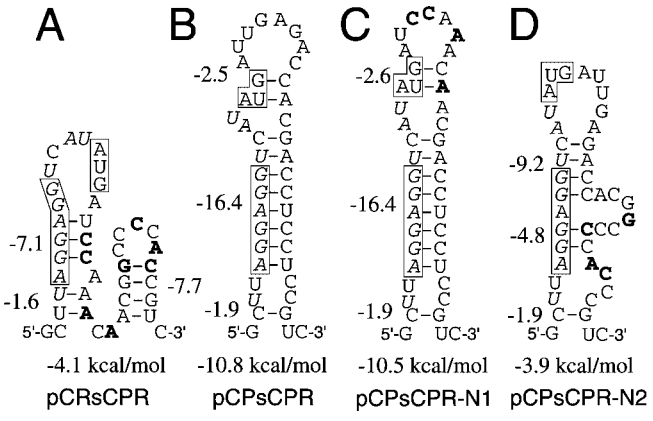

Fig. 3. **Putative partial secondary structures of mRNAs derived from expression plasmids of wild-type and chimeric sCPRs.** The local secondary structures of mRNAs derived from pCRsCPR (A), pCPsCPR (B), pCPsCPR-N1 (C), and pCPsCPR-N2 (D) were predicted with the program GeneBee (*34*, *35*). Nucleotides complementary with the 3′-terminal region of 16S rRNA are shown in italics. The hypothetical RBS (AGGAGG) and initiation codon (AUG) are boxed. In A, C, and D, nucleotides that differ from the corresponding nucleotides in the mRNA derived from pCPsCPR (B) are in bold letters. The names of the plasmids producing the mRNAs and their predicted overall stabilities (Δ*G*) are shown under the secondary structures. The values beside the stems are the stabilities of the stems (kcal/mol).

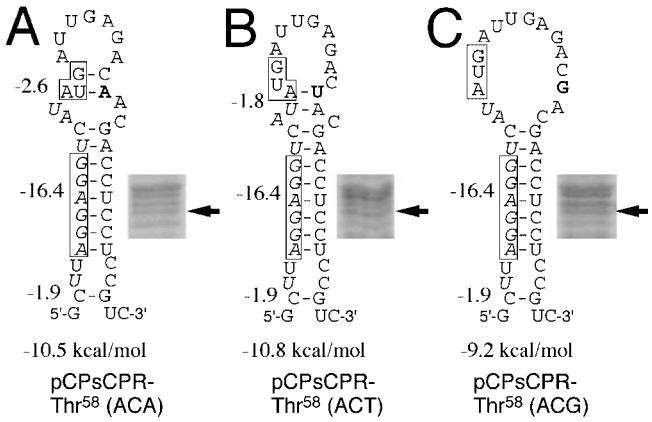

Fig. 4. **Putative partial secondary structures of the silently mutated mRNAs at the Thr^{58} codon in PsCPR and their corresponding protein expressions.** Protein expression of wild-type PsCPR and the local secondary structures of mRNAs derived from pCPsCPR-Thr^{58}(ACA) (A), -Thr^{58}(ACT) (B), and -Thr^{58}(ACG) (C). In the secondary structures, nucleotides that are complementary to the 3′-terminal region of the 16S rRNA are shown in italics. The hypothetical RBS (AGGAGG) and the initiation codon (AUG) are boxed. Nucleotides at the substituted positions are in bold letters. The names of the plasmids that produce the mRNAs and their predicted overall stabilities (Δ*G*) are shown under the secondary structures. The values beside the stems are the stabilities of the stems (kcal/mol). CBB-stained 7.5% polyacrylamide gels loaded with whole cell extracts of *E. coli* cells cultivated for 8 h in the presence of 0.2 mM IPTG are shown to the right of the secondary structure. The *E. coli* whole cell extract from 25 μl culture fluid was analyzed. The arrows indicate the position of the PsCPR band.

cells. Extracts of *E. coli* BL21/pCRsCPR cells cultivated in the absence of IPTG did not show an obvious RsCPR band on the CBB-stained gel (Fig. 2A, lane 2), but showed an obvious immuno-stained band (Fig. 2B, lane 2). This indicates that a low level of RsCPR protein accumulates in uninduced cultures. Whole cell extracts of *E. coli* BL21/pCPsCPR did not show an obvious band at the same position as purified RsCPR on the SDS-PAGE gel after cultivation either in the presence or absence of IPTG (Fig. 2A, lanes 4 and 5). However, cells cultivated in the presence of IPTG showed a thin immuno-stained band at a position similar to that of purified RsCPR (Fig. 2B, lane 5). This result indicates that a very low level of PsCPR accumulated in induced cells.

Expression of the PsCPR-N1and PsCPR-N2 Genes—In order to analyze whether or not the differences in the nucleotides encoding the N-terminal regions of PsCPR and RsCPR contribute to the accumulation of protein in *E. coli* cells, plasmids expressing chimeric PsCPR mutants, pCPsCPR-N1 and pCPsCPR-N2, were constructed (Fig. 1). Whole cell extracts of *E. coli* cells containing pCPsCPR-N1 (BL21/pCPsCPR-N1) showed no obvious band at the same position as that of purified RsCPR on the SDS-PAGE gel after cultivation either with or without IPTG (Fig. 2A, lanes 6 and 7). However, a thin band was detected by Western blot analysis of whole cell extracts after cultivation in the presence of IPTG (Fig. 2B, lane 7). This indicates that the accumulation level of PsCPR-N1 in *E. coli* cells was as low as that of the PsCPR from pCPsCPR. However, *E. coli* cells containing pCPsCPR-N2 (BL21/pCPsCPR-N2) showed an obvious band on the SDS-PAGE gel at the same position as that of the RsCPR after cultivation both in the presence and absence of IPTG (Fig. 2A, lanes 8 and 9). These bands were also detected by Western blot analysis (Fig. 2B, lanes 8 and 9). These results indicate that differences between the amino acid and/or the corresponding nucleotide sequences of Thr^{60}Ser^{61}Ser^{62} (ACCUCCUCC) in PsCPR and those of Ala^{60}Pro^{61}Pro^{62} (GCCCCACCC) in RsCPR are critical to protein accumulation.

Secondary Structure Predictions of the mRNAs for the Wild-type and Chimeric sCPRs—The local secondary structures of the mRNAs derived from pCRsCPR, pCPsCPR, pCPsCPR-N1, and pCPsCPR-N2 at the region shown in Figure 1 were predicted (Fig. 3). In the secondary structure of the mRNA derived from pCRsCPR, which resulted in a high-level of accumulation of RsCPR, the initiation codon (AUG) is unpaired in the loop, and the nucleotides in the hypothetical RBS (AGGAGG at position –10 to –5) form 3 base pairs with the UCC encoding the N-terminal region of RsCPR (Fig. 3A). In the secondary structure of the mRNA from pCPsCPR, which resulted in the accumulation of very little PsCPR, the initiation codon is base-paired with the CA in the Thr^{58}Thr^{59} codons, and the hypothetical RBS was in a long double strand. This double strand is composed of both the AGGAGGUC containing the RBS and the GACCUCCU in the codons for Thr^{59}Thr^{60}Ser^{61}Ser^{62} in PsCPR (Fig. 3B). The overall local secondary structure of the mRNA from pCPsCPR-N1 is similar to that from pCPsCPR, although slight structural differences are observed at the region from the second nucleotide (U) in the initiation codon to the first nucleotide (A) in the Thr^{59} codon (Fig. 3C). The long continuous double strand made of the AGGAGGUC is identical to that of pCPsCPR. The predicted secondary

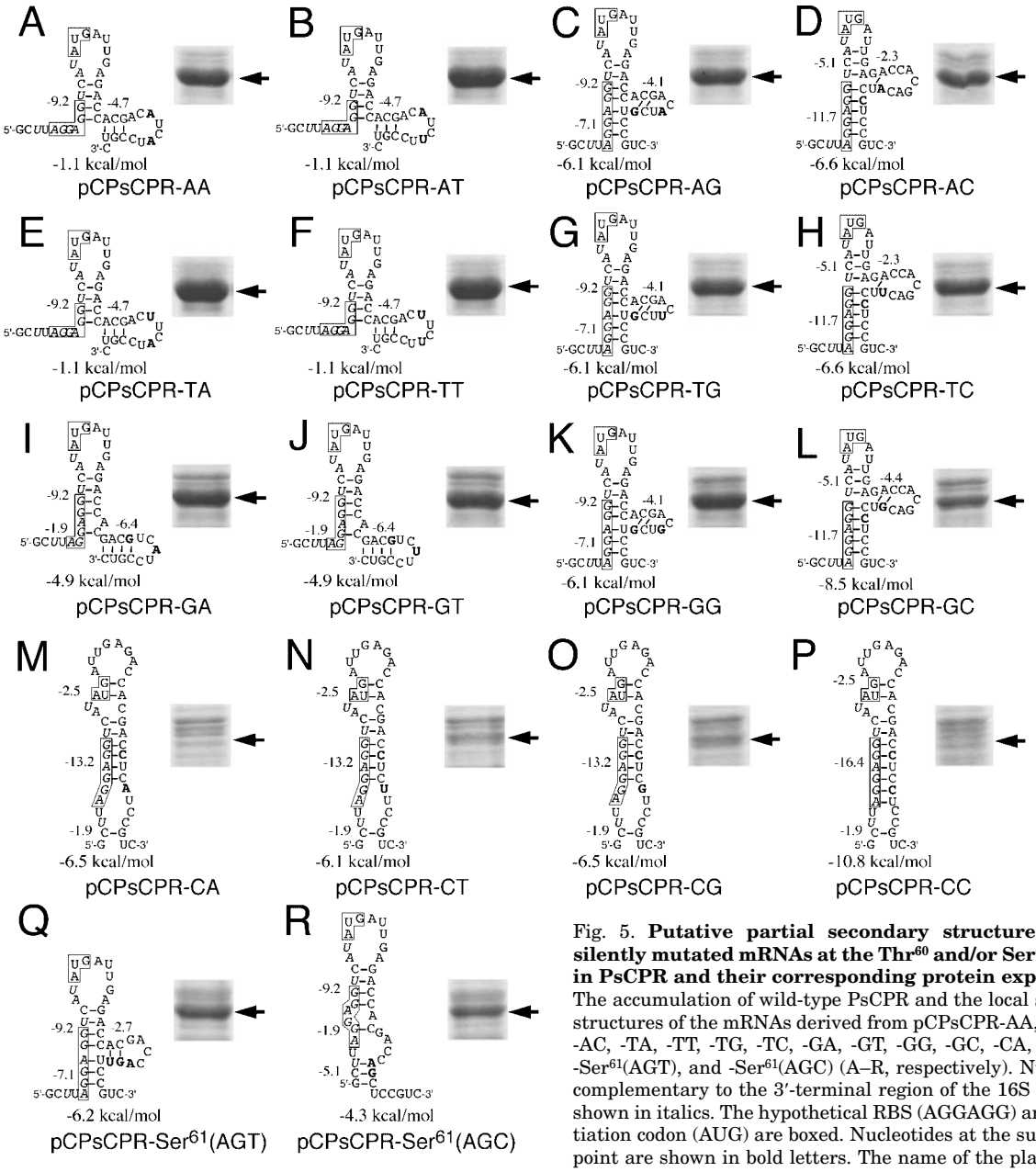

Fig. 5. **Putative partial secondary structures of the silently mutated mRNAs at the Thr^{60} and/or Ser^{61} codons in PsCPR and their corresponding protein expressions.** The accumulation of wild-type PsCPR and the local secondary structures of the mRNAs derived from pCPsCPR-AA, -AT, -AG, -AC, -TA, -TT, -TG, -TC, -GA, -GT, -GG, -GC, -CA, -CT, -CC, -Ser^{61}(AGT), and -Ser^{61}(AGC) (A–R, respectively). Nucleotides complementary to the 3′-terminal region of the 16S rRNA are shown in italics. The hypothetical RBS (AGGAGG) and the initiation codon (AUG) are boxed. Nucleotides at the substitution point are shown in bold letters. The name of the plasmid that produced the mRNA and the predicted overall stability (ΔG) are shown under the secondary structure. The values beside the stems are the stabilities of the stems (kcal/mol).

structure of the mRNA from pCPsCPR-N2, which caused high-level accumulation of the protein, is different from those of the mRNAs from the other three plasmids (Fig. 3D). The initiation codon is unpaired in the loop, and the two GGs in the hypothetical RBS form short double strands with a bulge of the ACGGCC encoding Thr^{59}Ala^{60}. These structures indicate that the intramolecular complementations between the RBS and the nucleotide sequences encoding the N-terminal region of the protein in the mRNAs from pCPsCPR and pCPsCPR-N1 are higher than those of the mRNAs from pCRsCPR and pCPsCPR-N2. It was concluded that the secondary structure at the RBS and/or the initiation codon in the mRNA have a significant effect on protein synthesis, and that the unpaired loop-out of the initiation codon and/or the destruction of the long stem containing the RBS in the mRNA from pCPsCPR-N2 cause the high-level accumulation of PsCPR-N2 in *E. coli*.

Expression of the PsCPR Genes Containing Silent Mutations at Thr^{58}—In order to analyze the effect of base-pairing at the initiation codon on the accumulation level of PsCPR, the expression plasmids pCPsCPR-Thr^{58}(ACA), -Thr^{58}(ACT), and -Thr^{58}(ACG) were constructed (Fig. 1). The predicted local secondary structure of the mRNA from pCPsCPR-Thr^{58}(ACA) is similar to that of pCPsCPR-N1 (Fig. 3C), and the base-pairing of UG in the initiation codon is maintained (Fig. 4A). The initiation codon in the mRNA from pCPsCPR-Thr^{58}(ACT) forms only one A-U

Table 1. **Accumulation levels of PsCPR and overall stabilities of the predicted secondary structures of the silently mutated mRNAs of PsCPR.**

Plasmid	Codon[a]		Accumulation[b] (%)	ΔG[c] (kcal/mol)
	Thr^{58}	$Thr^{60}Ser^{61}$		
pCPsCPR	ACC	ACCUCC	4	–10.8
pCPsCPR-Thr^{58} (ACA)	--A	------	4	–10.5
-Thr^{58} (ACT)	--U	------	14	–10.8
-Thr^{58} (ACG)	--G	------	12	–9.2
-AA	---	--A--A	75	–1.1
-AT	---	--A--U	94	–1.1
-AG	---	--A--G	73	–6.1
-AC	---	--A---	58	–6.6
-TA	---	--U--A	97	–1.1
-TT	---	--U--U	100	–1.1
-TC	---	--U---	80	–6.6
-TG	---	--U--G	75	–6.1
-GA	---	--G--A	91	–4.9
-GT	---	--G--U	81	–4.9
-GG	---	--G--G	87	–6.1
-GC	---	--G---	48	–8.5
-CA	---	-----A	11	–6.5
-CT	---	-----U	29	–6.1
-CG	---	-----G	29	–6.5
-CC	---	------	1	–10.8
-Ser^{61} (AGT)	---	---AGU	64	–6.2
-Ser^{61} (AGC)	---	--AG--	58	–4.3

[a]Codon in the mRNA from the plasmid indicated in the left column. Bar (–) represents nucleotides identical to those in the mRNA from pCPsCPR. [b]Accumulation level of PsCPR in *E. coli* cells relative to the expression level in BL21/pCPsCPR-TT cells, as estimated from the CBB-stained gel after SDS-PAGE. Errors in the densitometry determined for the band of PsCPR in BL21/pCPsCPR-TT cells were within ±5% (±S.E. of three measurements). [c]Overall stability of the predicted local secondary structures shown in Figs. 4 and 5.

base pair (Fig. 4B). In the mRNA from pCPsCPR-Thr^{58}(ACG), the initiation codon is unpaired in the loop (Fig. 4C). In these three structures, the long double stranded stem, which is made of AGGAGGUC, is identical to that from pCPsCPR.

Extracts of IPTG-induced *E. coli* cells containing pCsCPR-Thr^{58}(ACA) [BL21/pCPsCPR-Thr^{58}(ACA)], -Thr^{58}(ACT) [BL21/pCPsCPR-Thr^{58}(ACT)], and -Thr^{58}(ACG) [BL21/pCPsCPR-Thr^{58}(ACG)], showed very faint bands on the SDS-PAGE gel at a position corresponding to purified PsCPR (Fig. 4). The accumulation levels of PsCPR in these cells as estimated from the intensity of the bands are similar to that in BL21/pCPsCPR cells (Table 1). These results indicate that the silent mutations in the Thr^{58} codon, which were predicted to affect the base-pairing of the initiation codon, are not critical to the accumulation level of PsCPR.

Expression of the PsCPR Genes Containing Silent Mutations at $Thr^{60}Ser^{61}$—In order to compare the contribution of the intramolecular double strand composed of AGGAGGUC in the mRNA to the accumulation level of the PsCPR in *E. coli* cells, plasmids pCPsCPR-NN and -Ser^{61}(AGY) were constructed (Fig. 1). The PsCPR band on the SDS-PAGE gels and the relative accumulation levels of PsCPR in the cells containing these plasmids are shown in Fig. 5 and Table 1, respectively. The accumulation levels of PsCPR in *E. coli* BL21/pCPsCPR-AT, -TA, and -TT cells were very high, while those in *E. coli* BL21/pCPsCPR-CA, -CT, -CG, and -CC cells were less than 30% of that in BL21/pCPsCPR-TT cells. In the other cells, the accumulation levels varied from 48 to 91% of that in BL21/pCPsCPR-TT cells. These results indicate that the introduction of the silent mutations into the $Thr^{60}Ser^{61}$ codons is effective in changing the accumulation level of PsCPR.

Secondary Structures of the Silently Mutated mRNAs—The shapes of the predicted local secondary structures of mRNAs derived from pCPsCPR-CA, -CT, and -CG (Fig. 5 M–O) are similar to that of the mRNA from pCPsCPR, which can be designated as pCPsCPR-CC (Fig. 5P). In these three secondary structures, the base-pairing of the initiation codon and the 6 bp of continuous double strand containing GAGGUC are conserved, although the base pairs at the AG in the hypothetical RBS are eliminated due to the silent mutations at the Ser^{61} codon. In contrast, the shapes of the predicted secondary structures from the other plasmids are markedly changed (Fig. 5 A–L, Q, and R). In these secondary structures, the initiation codon is unpaired in the loop, and the continuous long double strand containing the AGGAGGUC shown in that of pCPsCPR-CC is shortened or divided by the bulge structure. These results suggest that the modulation of the intramolecular continuous double strand made of the AGGAGGUC, which contains the hypothetical RBS, significantly affects the accumulation level of PsCPR in *E. coli* cells.

Purification and Spectral Properties of PsCPR—Wild-type PsCPR was purified to homogeneity from the soluble

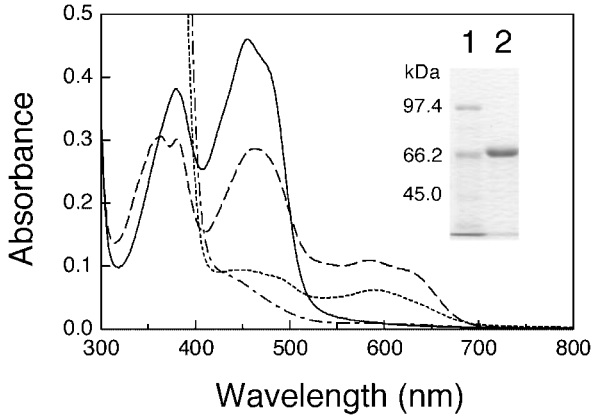

Fig. 6. **Absorption spectra and SDS-PAGE of the purified PsCPR.** Absorption spectra were measured after the sequential addition of 30 μM NADPH (broken line), 1 mM NADPH (dotted line), and an excess amount of sodium dithionite to the oxidized form of purified PsCPR (solid line) in 100 mM potassium phosphate (pH 7.0) containing 1 mM EDTA under aerobic conditions at 25°C. The protein concentration was 20 μM. Inset is the 10% polyacrylamide gel stained with CBB after SDS-PAGE. One microgram of PsCPR purified from *E. coli* BL21/pCPsCPR-TT cells (lane 2) was subjected to electrophoresis with SDS-PAGE Molecular Weight Standards (Bio-Rad) (lane 1).

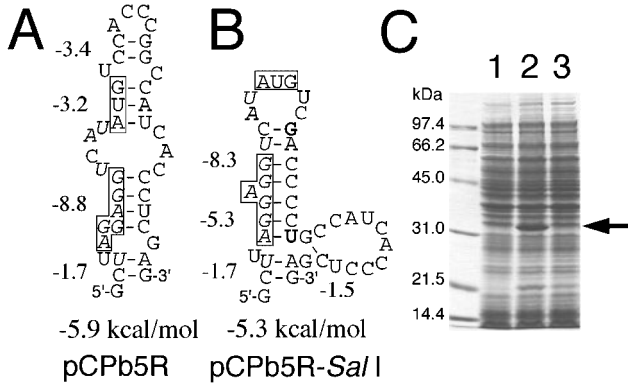

Fig. 7. **Putative partial secondary structures of the mRNAs for Psb5R and their corresponding protein expressions.** The local secondary structures of mRNAs derived from pCPb5R (A) and pCPb5R-*Sal*I (B), and a 12% polyacrylamide gel stained with CBB after SDS-PAGE (C). The representations of A and B are the same as those in the legend to Fig. 4. In C, whole cell extracts of *E. coli* BL21/pCPb5R (lanes 1 and 2), and pCPb5R-*Sal*I (lane 3) that were cultivated for 8 h in the absence (lane 1) and presence of 0.2 mM IPTG (lanes 2 and 3) were subjected to electrophoresis with SDS-PAGE Molecular Weight Standards (Bio-Rad). The arrow shows the position of the Psb5R band.

fraction of *E. coli* BL21/pCPsCPR-TT cells (Fig. 6, inset). The yield of purified PsCPR from 1 liter of culture fluid was 45.8 mg. The absorption spectra of the oxidized PsCPR and the spectral changes caused by the addition of NADPH are shown in Fig. 6. The oxidized PsCPR had absorption peaks at 380 nm and 455 nm with a shoulder at approximately 480 nm. After the addition of 30 μM NADPH, the air-stable semiquinone, which showed a broad peak at 585 nm and a shoulder at approximately 625 nm, was observed. The air-stable semiquinone, which was not completely reduced by excess NADPH, was completely reduced by excess sodium dithionite. These spectral changes in purified PsCPR are characteristic of CPR (*36–38*).

Expression of the Psb5R Genes Containing Silent Mutations at Ser[1] and Pro[3]—The plasmid pCPb5R (*18*), which is a derivative of pCW_{ori}^{+} (Fig. 1), highly expresses Psb5R after induction with IPTG (Fig. 7C, lanes 1 and 2). In the predicted local secondary structure of the mRNA from the plasmid pCPb5R, the initiation codon is base-paired, and the GAGG in the hypothetical RBS and CU forms base pairs (Fig. 7A). We found that the silent mutations converting UCC to UCG at the Ser[1] codon and CCC to CCU at the Pro[3] codon made the predicted local secondary structure at the RBS in mRNA much more stable. The expression plasmid for Psb5R containing these silent mutations was named pCPb5R-*Sal*I (Fig. 1). In the predicted secondary structure of the mRNA from pCPb5R-*Sal*I, the initiation codon is unpaired, and the 7 bp of long stem contains base-paired AGG and GG and an unpaired A in the RBS (Fig. 7B). *E. coli* BL21 cells containing pCPb5R-*Sal*I showed only a weak Psb5R band after induction with IPTG (Fig. 7C, lane 3). This indicates that the silent mutations employed here significantly decrease the accumulation level of Psb5R in *E. coli* cells.

DISCUSSION

In this study, we cloned and expressed the cDNA encoding PsCPR in *E. coli* cells using pCW_{ori}^{+}. The accumulation level of PsCPR in *E. coli* BL21/pCPsCPR cells was very low, while that of RsCPR in BL21/pCRsCPR cells was very high (Fig. 2). The observed expression of the chimeric proteins PsCPR-N1 and -N2 suggests that the differences between the amino acid and/or corresponding nucleotide sequences of $Thr^{60}Ser^{61}Ser^{62}$ in PsCPR and those of $Ala^{60}Pro^{61}Pro^{62}$ in RsCPR are critical to protein accumulation (Fig. 2). We have been successful in expressing wild-type PsCPR at high levels by introducing silent mutations at the $Thr^{60}Ser^{61}$ codons. Purified PsCPR from *E. coli* BL21/pCPsCPR-TT showed spectral changes characteristic of sCPR (Fig. 7). This high-level PsCPR expression system is expected to be useful for analyzing the electron transfer system in porcine liver.

It is well known that the expression of heterologous proteins in *E. coli* cells is dependent on a number of factors at both the transcriptional and translational levels, and on the stability of the synthesized protein against proteolysis in cells. Since the silently mutated PsCPR genes encode the same protein, the accumulation level of the silently mutated PsCPR does not depend on the stability of the synthesized protein. The strong tandem *tac* promoters in pCW_{ori}^{+} produce high amounts of mRNA, and some heterologous proteins are highly expressed even in the absence of IPTG. For example, we have observed that Psb5 was highly expressed in the absence of IPTG using pCPb5 (*20*), which is a derivative of pCW_{ori}^{+} (data not shown). This is probably due to a shortage of the repressor in *E. coli* cells. The expression of PsCPR-N2 in the absence of IPTG (Fig. 2) may also be due to the same factor. Therefore, it was concluded that transcription of the PsCPR genes is not the rate-limiting step of protein synthesis and that the variations in the

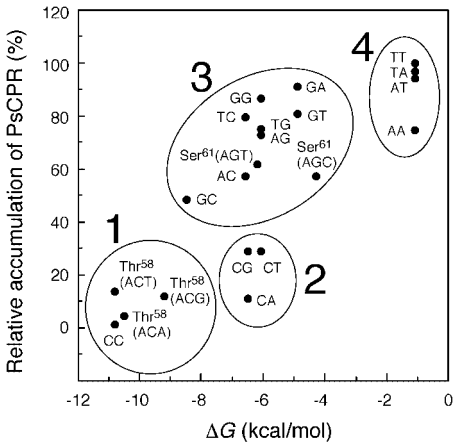

Fig. 8. **Quantitative relationship between the relative accumulation of PsCPR and the overall local stability of the mRNA.** The relative accumulation levels of PsCPR were plotted against the overall local secondary structure stabilities (Δ*G*) with the name of the corresponding plasmid, from which pCPsCPR- is omitted. The plots are classified into groups 1–4 (surrounded by solid lines) based on the plotted area and the shape of the predicted secondary structure of the mRNA.

accumulation of the silently mutated PsCPR presented here are due to differences at the translational level.

The predicted local secondary structures of the mRNAs from pCRsCPR, pCPsCPR, -N1, and -N2 suggest that the secondary structure at the initiation codon and/or the RBS in the mRNA significantly affect protein accumulation in *E. coli* cells. The importance of base pairing at the initiation codon in determining efficient translation has been pointed out (*39*, *40*). However, the silent mutations at the Thr^{58} codon in PsCPR, which modulates base-pairing at the initiation codon without changing the long stem containing AGGAGGUC, hardly changed the expression level of the protein (Fig. 4). The expression levels of PsCPR in *E. coli* BL21/pCPsCPR-CT and -CG cells were higher than that in BL21/pCPsCPR cells, although the base-pairing of the initiation codon in the mRNA was not changed by the silent mutations (Fig. 5 N–P). In the case of Psb5R expression, the silent mutation at the Ser^{1} and Pro^{3} codons in Psb5R, which eliminate the base pairs at the initiation codon, decreased the expression of PsCPR (Fig. 7). It is concluded that the local secondary structure at the RBS rather than base-pairing at the initiation codon is critical for determining the expression. This conclusion is consistent with the suggestion by de Smit and van Durin (*41*) that the stability of the secondary structure at the RBS is important for the control of translation in *E. coli* cells, whether or not the initiation codon itself is base-paired. It is well known that the 3′-terminal region of the 16S rRNA complementarily recognizes the RBS in mRNA in the initial stage of translation in *E. coli* cells. This recognition is necessary for the construction of the ribosome particle on the mRNA molecule. Therefore, the formation of a stable intramolecular secondary structure at the RBS in mRNA can disturb the complementary recognition by 16S rRNA, resulting in a decrease in the expression level of the protein (*7*, *41–43*). In the case of pCPsCPR, the stable double strand containing the AGGAGG at the hypothetical RBS probably resulted in the significant decrease in the accumulation level of PsCPR. Etchegaray and Inouye (*44*) demonstrated that the downstream box, which is complementary to bases 1469–1483 in the *E. coli* 16S rRNA (*45*, *46*), also plays a major role in the enhancement of translation initiation in concert with the Shine-Dalgarno sequence. However, the nucleotide sequence of the downstream box was not found in the mRNAs presented here.

The calculated stabilities (Δ*G*) of the overall local secondary structures of the silently mutated mRNAs encoding PsCPR varied from –1.1 to –10.8 kcal/mol (Table 1). de Smit and van Durin (*41*) reported that the efficiency of translation is determined by the overall stability of the structure at the RBS based on the quantitative analysis of the secondary structure of the mRNA and expression levels of the coat-protein gene from bacteriophage MS2 (*43*), the *lamB* gene of *E. coli* (*47*), human somatomedin-C gene (*48*), the *mom* gene of bacteriophage Mu (*49*, *50*), and the transposase gene encoded by the IS50 insertion sequence in *E. coli* cells (*51*). The correlation between the overall stabilities and accumulation levels of PsCPR is shown in Fig. 8. Indeed, it seems that the accumulation levels roughly depend on the overall local stability of the mRNA. However, it is noted that the mRNAs can be classified into 4 groups based on the plotted area in Fig. 8 and the shapes of the predicted secondary structures of the mRNA as follows. The first group (group 1) includes the mRNAs from pCPsCPR-CC, -Thr^{58}(ACA), -Thr^{58}(ACT), and -Thr^{58}(ACG). In this group, the entire hypothetical RBS (AGGAGG) is involved in a continuous double strand made of AGGAGGUC (Figs. 4 and 5P). The calculated local stability of the double strand is –16.4 kcal/mol. The second group (group *2*) includes the mRNAs from pCPsCPR-CA, -CT, and -CG. In this group, the 5′-terminal AG in the RBS is unpaired and the remaining bases (GAGG) are involved in a continuous double strand made of GAGGUC (Fig. 5 M–O). The local stability of this continuous double strand is –13.2 kcal/mol, which is more unstable than that in group 1. The accumulation levels of PsCPR from the mRNAs in group 2 are similar to those in group 1. The third group (group 3) includes the mRNAs from pCPsCPR-AG, -AC, -TG, -TC, -GA, -GT, -GG, -GC, -Ser^{61} (AGT), and -Ser^{61}(AGT) (Fig. 5 C, D, G, H, I–L, Q, and R), and the last group (group 4) includes the mRNAs from pCPsCPR-AA, -AT, -TA, and -TT (Fig. 5 A, B, E, and F). In groups 3 and 4, the continuous double strand containing the RBS in the mRNA, which was predicted in group 1, is shortened and/or divided by the additional stem and loop structure, and the accumulation levels are higher than those of groups 1 and 2. In the mRNAs of group 1, the overall stabilities of the predicted secondary structures are –1.1 kcal/mol, more than 3 kcal/mol less stable than those in group 3. These results suggest that the accumulation level of PsCPR depends on the stability of the continuous double strand structure at the RBS rather than the predicted overall stability calculated here.

It is of interest that the expression level of PsCPR in *E. coli* BL21/pCPsCPR-GC was obviously lower than in BL21/pCPsCPR-AC and -TC, although the shapes of the predicted local secondary structures of the mRNAs are very similar (Fig. 5 D, H, and L). In the mRNA from pCPsCPR-GC, there is an additional G-C pair between

the second base (C) in the Thr^{58} codon and the third base (G) in the Thr^{60} codon in the stem of the bulge, which is inserted into the double strand containing the GAG-GCUA (Fig. 5L). This additional G-C pair may affect the expression level of PsCPR. The local stabilization effect of this G-C pair is approximately 2 kcal/mol, a value large enough to change the expression level, because de Smit and van Durin (*41*, *43*) demonstrated that protein expression levels decrease approximately 10-fold for each –1.5 kcal/mol.

In this study, we have not only increased the expression of PsCPR but also decreased the expression level of Psb5R by designing silent mutations based on mRNA secondary structure predictions (Figs. 5 and 7). The modulation of the intramolecular local secondary structure at the RBS in an mRNA is a useful approach to control the expression level of proteins. This approach was effective when using an expression plasmid such as pCW_{ori}^{+}, which contains strong promoters. The control of protein expression may be useful for constructing high-level coexpression systems for cofactor proteins, such as the coexpression of inducible nitric oxide synthase with calmodulin (*52*), by modulating expression levels of the individual proteins.

The use of local secondary structure prediction at the region containing the RBS in an mRNA is very helpful for selecting candidate bases for mutation. The predicted local secondary structures of the mRNA from pCPsCPR depend on the length and position of the nucleotide sequences used for the prediction. The secondary structure prediction of the mRNA from pCPsCPR using the nucleotide sequences from –12 to +24 and from –26 to +51 showed a continuous double stranded structure composed of AGGAGGUC (identical to that shown in Fig. 3B), although the overall secondary structures were changed (data not shown). These results suggest that the continuous local double strand at the RBS, which decreased the expression level of the protein, was accurately predicted with the prediction program employed here.

In conclusion, we have constructed a high-level expression system for PsCPR by modulating the predicted local secondary structure of the RBS. The expression level of PsCPR depended on the local stability of the secondary structure of the mRNA at the RBS rather than the overall local stabilities of the predicted secondary structure. The data presented here demonstrate that the introduction of silent mutations based on the predicted local secondary structure at the RBS in mRNA is a useful approach to control and increase the expression level of heterologous proteins in *E. coli* cells.

We thank Dr. Yoshikazu Emi and Dr. Shin-ichi Ikushiro for helpful discussions, and Mr. Hiroshi Toyota, Ms. Miwa Hisamori, and Ms. Kaori Hada for technical assistance. This work was supported in part by a Grant-in-Aid, number 11169235, and by COE 21 from the Ministry of Education, Culture, Sports, Science, and Technology of Japan.

REFERENCES

1. Makrides, S.C. (1996) Strategies for achieving high-level expression of genes in *Escherichia coli*. *Microbiol. Rev.* **60**, 512–538
2. Balbas, P. and Boliver, F. (1985) Design and construction of expression plasmid vectors in *Escherichia coli* in *Methods Enzymol.*, *vol. 185 Gene Expression Technology* (Goeddel, D.V., ed.), pp. 14–37, Academic Press, San Diego
3. Winnacker, E.-L. (1987) Expression vectors in prokaryotes in *From genes to clones: Introduction to Gene Technology* (Ibelgaufts, H. transl.) pp. 239–267, VCH Publishers, New York
4. Shine, J. and Dalgarno, L. (1974) The 3′-terminal sequence of *Escherichia coli* 16S ribosomal RNA: complementarity to nonsense triplets and ribosome binding sites. *Proc. Natl Acad. Sci. USA* **71**, 1342–1346
5. Schoner, B.E., Hsiung, H.M., Belagaje, R.M., Mayne, N.G., and Schoner, R.G. (1984) Role of mRNA translational efficiency in bovine growth hormone expression in *Escherichia coli*. *Proc. Natl Acad. Sci. USA* **81**, 5403–5407
6. Schoner, B.E., Belagaje, R.M., and Schoner, R.G. (1986) Translation of a synthetic two-cistron mRNA in *Escherichia coli*. *Proc. Natl Acad. Sci. USA* **83**, 8506–5810
7. Puri, N., Rao, K.B.C.A., Menon, S., Panda, A.K., Tiwari, G., Grag, L.C., and Totey, S.M. (1999) Effect of the codon following the ATG start site on the expression of bovine growth hormone in *Escherichia coli*. *Protein Expression Purif.* **17**, 215–223
8. Johansson, A.-S., Bolton-Grob, R., and Mannervik, B. (1999) Use of silent mutations in cDNA encoding human glutathione transferase M2-2 for optimized expression in *Escherichia coli*. *Protein Expression Purif.* **17**, 105–112
9. Hrzenjak, A., Artl, A, Knipping, G., Kostner, G., Sattler, W., and Malle, E. (2001) Silent mutations in secondary Shine-Dalgarno sequences in the cDNA of human serum amyloid A4 promotes expression of recombinant protein in *Escherichia coli*. *Protein Eng.* **14**, 949–952
10. Shen, A. and Kasper, C.B. (1993) Protein and gene and regulation of NADPH cytochrome P450 oxidoreductase. in *Handbook of Experimental Pharmacology*, *Volume 105: Cytochrome P450* (Schenkman, J.B. and Graim, H., eds.) pp. 35–59, Springer-Verlag, Berlin
11. Iyanagi, T. and Mason, H.S. (1973) Some properties of hepatic reduced nicotinamide adenine dinucleotide phosphate-cytochrome *c* reductase. *Biochemistry* **12**, 2297–2308
12. Takano, T., Bando, S., Horii, C., Higashiyama, M., Ogawa, K., Sato, M., Katsuya, Y., Dannno, M., Yubisui, T., Shirabe, K., and Takeshita, M. (1994) The structure of human erythrocite NADH-cytochrome b_5 reductase at 2.5 Å resolution in *Flavins and Flavoproteins* (Yagi, K., ed.) pp. 409–412, Walter de Gruyter, Berlin
13. Nishida, H., Inaka, K., Yamanaka, M., Kaida, S., Kobayashi, K., and Miki, K. (1995) Crystal structure of NADH-cytochrome b_5 reductase from pig liver at 2.4 Å resolution. *Biochemistry* **34**, 2763–2767
14. Bewley, M.C., Marohnic, C.C., and Barber, M.J. (2001) The structure and biochemistry of NADH-dependent cytochrome b_5 reductase are now consistent. *Biochemistry* **40**, 13574–13582
15. Wu, J., Gan, J.H., Xia, Z.X., Wang, Y.H., Wang, W.H., Xue, L.L., Xie, Y., and Huang, Z.X. Crystal structure of recombinant trypsin-solubilized fragment of cytochrome b_5 and the structural comparison with Val61His mutant. (2000) *Proteins* **40**, 249–257
16. Wang, M., Roberts, D.L., Paschke, R., Shea, T.M., Masters, B.S.S., and Kim, J.J.P. Three-dimensional structure of NADPH-cytochrome P450 reductase: prototype for FMN- and FAD-containing enzymes. (1997) *Proc. Natl Acad. Sci. USA* **94**, 8411–8416
17. Shirabe, K., Yubisui, T., and Takeshita, M. (1994) Role of flavin binding motif, RxY(T/S) of NADH-cytochrome b_5 reductase in electron transfer reaction in *Flavins and Flavoproteins* (Yagi, K., ed.) pp. 405–408, Walter de Gruyter, Berlin

18. Kimura, S., Emi, Y., Ikushiro, S., and Iyanagi, T. (1999) Systematic mutations of highly conserved His^{49} and carboxyl-terminal of recombinant porcine liver NADH-cytochrome b_5 reductase solubilized domain. *Biochim. Biophys. Acta* **1430**, 290–301
19. Kimura, S., Nishida, H., and Iyanagi, T. (2001) Effects of flavin-binding motif amino acid mutations in the NADH-cytochrome b_5 reductase catalytic domain on protein stability and catalysis. *J. Biochem.* **130**, 481–490
20. Kimura, S., Kawamura, M., and Iyanagi, T. (2003) Role of Thr^{66} in porcine NADH-cytochrome b_5 reductase in catalysis and control of the rate-limiting step in electron transfer. *J. Biol. Chem.* **278**, 3580–3589
21. Kawano, M., Shirabe, K., Nagai, T., and Takeshita M. (1998) Role of carboxyl residues surrounding heme of human cytochrome b_5 in the electrostatic interaction with NADH-cytochrome b_5 reductase. *Biochem. Biophys. Res. Commun.* **245**, 666–669
22. Shirabe, K., Nagai, T., Yubisui, T., and Takeshita, M. (1998) Electrostatic interaction between NADH-cytochrome b_5 reductase and cytochrome b_5 studied by site-directed mutagenesis. *Biochim. Biophys. Acta* **1384**, 16–22
23. Shen, A.L., Sem, D.S., and Kasper, C.B. (1999) Mechanistic studies on the reductive half-reaction of NADPH-cytochrome P450 oxidoreductase. *J. Biol. Chem.* **274**, 5391–5398
24. Gutierrez, A., Paine, M., Wolf, R., Scrutton, N.S., and Roberts, G.C.K. (2002) Relaxation kinetics of cytochrome P450 reductase: Internal electron transfer is limited by conformational change and regulated by coenzyme binding. *Biochemistry* **41**, 4626–4637
25. Bridges, A., Gruenke, L., Chang, Y.-T., Vakser, I.A., Loew, G., and Waskell, L. (1998) Identification of the binding site on cytochrome P450 2B4 for cytochrome b_5 and cytochrome P450 reductase. *J. Biol. Chem.* **273**, 17036–17049
26. Muchmore, D.C., McIntosh, L.P., Russell, C.B., Anderson, D.E., and Dahlquist, F.W. (1989) Expression and nitrogen-15 labeling of proteins for proton and nitrogen-15 nuclear magnetic resonance in *Methods Enzymol.*, *vol. 177 Nuclear Magnetic Resonance*, *Part B*, *Structure and Mechanism.* (Oppenheimer, N.J. and James, T.L., eds.), pp. 44–73, Academic Press, San Diego
27. Gegner, J.A. and Dahlquist, F.W. (1991) Signal transduction in bacteria: CheW forms a reversible complex with the protein kinase CheA. *Proc. Natl Acad. Sci. USA* **88**, 750–754
28. Barnes, H.J., Arlotto, M.P., and Waterman, M.R. (1991) Expression and enzymatic activity of recombinant cytochrome P450 17α-hydroxylase in *Escherichia coli*. *Proc. Natl Acad. Sci. USA* **88**, 5597–5601
29. McMillan, K. and Masters, B.S. (1995) Prokaryotic expression of the heme- and flavin-binding domains of rat neuronal nitric oxide synthase as distinct polypeptides: identification of the heme-binding proximal thiolate ligand as cysteine-415. *Biochemistry* **34**, 3686–3693
30. Matsuda, H. and Iyanagi, T. (1999) Calmodulin activates intramolecular electron transfer between the two flavins of neutral nitric oxide synthase flavin domain. *Biochim. Biophys. Acta* **1473**, 345–355
31. Haniu, M., Iyanagi, T., Miller, P., Lee, T.D., and Shively, J.E. (1986) Complete amino acid sequence of NADPH-cytochrome P-450 reductase from porcine hepatic microsomes. *Biochemistry* **25**, 7906–7911
32. Vogel, L. and Lumper, L. (1986) Complete structure of the hydrophilic domain in the porcine NADPH-cytochrome P-450 reductase. *Biochem. J.* **236**, 871–878
33. Porter, T.D. and Kasper, C.B. (1985) Cloning nucleotide sequence of rat NADPH-cytochrome P-450 oxidoreductase cDNA and identification of flavin-binding domains. *Proc. Natl Acad. Sci. USA* **82**, 973–977
34. Brodsky, L.I., Vasilyev, A.V., Kalaydzidis, Ya.L., Osipov, Yu.S., Tatuzov, A.R.L., and Feranchuk, S.I. (1992) GeneBee: the program package for biopolymer structure analysis. *Dimacs* **8**, 127–139
35. Brodsky, L.I., Ivanov, V.V., Kalaydzidis, Ya.L., Leontovich, A.M., Nikolaev, V.K. Feranchuk, S.I., and Drachev, V.A. (1995) GeneBee-NET: Internet-based server for analyzing biopolymers structure. *Biochemistry (Moscow)* **60**, 923–928
36. Iyanagi, T., Anan, F.K., Imai, Y., and Mason, H.S. (1978) Studies on the microsomal mixed function oxidase system: redox properties of detergent-solubilized NADPH-cytochrome P-450 reductase. *Biochemistry* **17**, 2224–2230
37. Iyanagi, T., Makino, R., and Anan, F.K. (1981) Studies on the microsomal mixed function oxidase system: Mechanism of action of hepatic NADPH-cytochrome P-450 reductase. *Biochemistry* **20**, 1722–1730
38. Matsuda, H., Kimura, S., and Iyanagi, T. (2000) One-electron reduction of quinines by the neuronal nitric-oxide synthase reductase domain. *Biochim. Biophys. Acta* **1459**, 106–116
39. Iselentent, D. and Fiers, W. (1980) Secondary structure of mRNA and efficiency of translation initiation. *Gene* **9**, 1–12
40. Gheysen, D., Iselentent, D., Derom, C., and Fiers, W. (1982) Systematic alteration of the nucleotide sequence preceding the translational initiation codon and the effects on bacterial expression of the cloned SV40 small t-antigen gene. *Gene* **17**, 55–63
41. de Smit, M.H. and de Duin, J. (1994) Control of translation by mRNA secondary structure in *Escherichia coli*. A quantitative analysis of literature data. *J. Mol. Biol.* **244**, 144–150
42. Hallewell, R.A., Masiarz, F.R., Najarian, R.C., Puma, J.P., and Quiroga, M.R. (1985) Human Cu/Zn superoxide dismutase cDNA: isolation of clones synthesizing high levels of active or inactive enzyme from an expression library. *Nucleic Acids Res.* **13**, 2017–2034
43. de Smit, M.H. and de Duin, J. (1990) Secondary structure of the ribosome binding site determines translational efficiency: A quantitative analysis. *Proc. Natl Acad. Sci. USA* **87**, 7668–7672
44. Etchegaray, J.-P. and Inouye, Y. (1999) Translational enhancement by an element downstream of the initiation codon in *Escherichia coli*. *J. Biol. Chem.* **274**, 10079–10085
45. Sprengart, M.L., Fatscher, H.P., and Fuchs, E. (1990) The initiation of translation in *E. coli*: apparent base pairing between the 16S rRNA and downstream sequences of the mRNA. *Nucleic Acids Res.* **18**, 1719–1723
46. Sprengart, M.L., Fuchs, E., and Porter, A.G. (1996) The downstream box: an efficient and independent translation initiation signal in *Escherichia coli*. *EMBO J.* **15**, 665–674
47. Hall, M.N., Gabay, J., Débarbouillé, M., and Schwartz, M. (1982) A role for mRNA secondary structure in the control of translation initiation. *Nature* **295**, 616–618
48. Buell, M.R., Schulz, M.-F., Selzer, G., Chollet, A., Movva, N.R., Semon, D., Escanez, S., and Kawashima, E. (1985) Optimizing the expression in *E. coli* of a synthetic gene encoding somatomedin-C (IGF-I). *Nucleic Acids Res.* **13**, 1923–1938
49. Wulczyn, F.G., Bölker, M., and Kahmann, R. (1989) Translation of the bacteriophage Mu *mom* gene is positively regulated by the phage *com* gene product. *Cell* **57**, 1201–1210
50. Wulczyn, F.G., and Kahmann, R. (1991) Translational stimulation: RNA sequence and structure requirements for binding of Com protein. *Cell* **65**, 259–269
51. Schulz, V.P. and Reznikoff, W.S. (1991) Translational initiation of IS*50*R read-through transcript. *J. Mol. Biol.* **221**, 65–80
52. Wu, C., Zhang, J., Abu-Soud, H., Ghosh, D.K., and Stuehr, D.J. (1996) High-level expression of mouse inducible nitric oxide synthase in *Escherichia coli* requires coexpression with calmodulin. *Biochem. Biophys. Res. Commun.* **222**, 439–444